# A generalized soft-sphere model for Monte Carlo simulation

Jing Fan

*Institute of Mechanics, Chinese Academy of Sciences, Beijing 100080, People's Republic of China*

A new collision model, called the generalized soft-sphere (GSS) model, is introduced. It has the same total cross section as the generalized hard-sphere model [Phys. Fluids A **5**, 738 (1993)], whereas the deflection angle is calculated by the soft-sphere scattering model [Phys. Fluids A **3**, 2459 (1991)]. In virtue of a two-term formula given to fit the numerical solutions of the collision integrals for the Lennard-Jones (6-12) potential and for the Stockmayer potential, the parameters involved in the GSS model are determined explicitly that may fully reproduce the transport coefficients under these potentials. Coefficients of viscosity, self-diffusion and diffusion for both polar and nonpolar molecules given by the GSS model and experiment are in excellent agreement over a wide range of temperature from low to high. © *2002 American Institute of Physics.*
[DOI: 10.1063/1.1521123]

## I. INTRODUCTION

The direct simulation Monte Carlo (DSMC) method is a general numerical technique to analyze rarefied gas flows.[1] The strategy of DSMC is to track the molecular trajectory and status based on the collision mechanics of model molecules, and then obtain physical quantities of interest through statistical average. A physically realistic collision model is therefore critical for DSMC to predict various gas flows reliably and accurately. In actual gases the force between two molecules is repulsive at small distances, and more weakly attractive at larger distances. This behavior is most simply described by the Lennard-Jones (6-12) potential[2,3]

$$\varphi(r) = 4\varepsilon \left[ \left( \frac{\sigma}{r} \right)^{12} - \left( \frac{\sigma}{r} \right)^{6} \right]. \qquad (1)$$

The parameters $\varepsilon$ and $\sigma$ (which have dimensions of energy and length, respectively) are constants characteristic of the chemical species of the colliding molecules, and $r$ is the inter-molecular separation. Systematic studies[2,3] showed that the potential (1) was adequate for a number of nonpolar molecules such as air.

For polar molecules like ammonia and water vapor, however, strong electrostatic interaction leads to anomalous behavior with respect to the potential (1).[2,3] This electrostatic contribution is proven proportional to the inverse third power of the intermolecular separation. Stockmayer combined such a term with the Lennard-Jones potential to describe the interaction between polar molecules[2,3]

$$\varphi(r) = 4\varepsilon \left[ \left( \frac{\sigma}{r} \right)^{12} - \left( \frac{\sigma}{r} \right)^{6} - \delta \left( \frac{\sigma}{r} \right)^{3} \right], \qquad (2)$$

where $\delta$ is a dimensionless constant that measures the polarization of a substance. The potential (2), known as the Stockmayer potential, was successfully applied to many polar molecules.[2,3]

An accurate procedure to calculate collision cross sections and scatter for the potentials (1) or (2) has been widely used in kinetic studies of transport properties.[2,3] Application of this procedure to DSMC, though straightforward in principle, is too computationally intensive in engineering context where millions and even billions of molecular collisions have to be considered. Many efforts[4–9] have been paid to establish a collision model appropriate to the DSMC method, such as the variable hard-sphere (VHS) model of Bird,[4,5] variable soft-sphere (VSS) model of Koura and Matsumoto,[7,8] and generalized hard-sphere (GHS) model of Hassan and Hash.[9] Besides the computational efficiency, these models aimed at phenomenological reproduction of transport coefficients under the inverse-power-law (IPL) or Lennard-Jones potential. They were to some extent successful, whereas certain important issues such as molecular polarization remain to be settled. Moreover, the parameters involved in the GHS and VSS models for the Lennard-Jones potential were not expressed explicitly, and had to be numerically solved through the least-square fitting of experimental data.[8,9] This is of course inconvenient for practical simulation.

This paper is organized as follows. First, previous models are reviewed. Then, a universal collision model, named as generalized soft-sphere (GSS) model, is introduced that is suitable to both polar and nonpolar molecules over a wide temperature range. By virtue of a fitting formula of the numerical solutions of the collision integrals for the potentials (1) and (2), the parameters involved in the GSS model are expressed explicitly. Next, transport coefficients given by GSS previous models are compared with experimental data. Finally, some conclusions are given.

## II. PREVIOUS MODELS

The VHS model[4,5] assumes that the total cross section varies like

$$\sigma_T \propto c_r^{-2\omega}, \qquad (3)$$

while the deflection angle in a collision follows the hard sphere scattering law, i.e., an isotropic scattering in the center-of-mass frame of reference

$$\chi = 2 \arccos(b/d), \tag{4}$$

where $c_r$ is the relative speed of the colliding molecules, and $b$ is the miss-distance impact parameter. The total cross section (3) bears the same relation of coefficient of viscosity to temperature as the IPL potential[1,4]

$$\mu \propto T^{\omega + 1/2}, \tag{5}$$

where $\omega = 2/(\eta - 1)$, and $\eta$ is the power of IPL.

It is well known that the IPL potential considers the repulsive force between molecules only and becomes poor at low temperatures where the attractive force dominates.[2,3] Therefore, it is desirable to establish a model based on potentials with both attraction and repulsion like (1). Under the hard-sphere scattering, the potential (1) has the relation of coefficient of viscosity to temperature as follows:[9]

$$\mu \propto \frac{T^{1/6 + 1/2}}{1 + c_o T^{-1/2}}, \tag{6}$$

where $c_o$ is a constant. Clearly, the relations (5) and (6) are inconsistent. This led to the introduction by Hassan and Hash[9] of the GHS model, in which the deflection angle obeys the hard-sphere scattering law (4), while the total collision cross section is described by more than one term

$$\frac{\sigma_T}{\sigma^2} = \sum \beta_j \left( \frac{E_t}{\varepsilon} \right)^{-\ell_j}, \tag{7}$$

where $E_t = \frac{1}{2} m_r c_r^2$, $m_r$ is the reduced mass of two colliding molecules, and $\beta_j$ and $\ell_j$ are constants that are determined through a numerically least-square fit of experimental data of viscosity coefficient for simple gases, and binary diffusion coefficient for gas mixtures. This is not only inconvenient, but sometimes even infeasible because the coefficients of diffusion are difficult to observe and experimental data are often not available.[3,11]

Koura and his co-workers[6,7] showed that the hard-sphere scattering law employed in the VHS and GHS models led to an unreal ratio of the momentum to viscosity cross-section. They suggested a soft-sphere scattering model to calculate the deflection angle[7]

$$\chi = 2 \arccos[(b/d)^{1/\alpha}], \tag{8}$$

where $b$ is the miss-distance impact parameter, $d$ is the collision diameter. The deflection angle (8) gives rise to the viscosity and momentum cross sections as follows:[7]

$$\sigma_\mu = \frac{2 S_\mu}{3} \sigma_T, \quad \sigma_\mu = S_D \sigma_T, \tag{9}$$

with $S_\mu = 6\alpha/[(\alpha+1)(\alpha+2)]$ and $S_D = 2/(\alpha+1)$.

In the VSS model,[7] the total cross section and $\alpha$ are chosen in such a way to reproduce the actual viscosity and diffusion cross sections for a given interaction potential

$$\alpha = (\sigma_D/\sigma_\mu - 0.5)^{-1}, \quad \sigma_T = \frac{3\sigma_\mu}{2 S_\mu}. \tag{10}$$

For the IPL potential, the analytical expressions of $\sigma_\mu$ and $\sigma_D$ are available,[2,3] from which $\sigma_T$ and $\alpha$ are easily derived:[7] $\sigma_T$ has the same relation to $c_r$ as the VHS model, and $\alpha$ is a constant dependent upon the molecular species. The values of $\alpha$ for a number of gases were given in Table I of Ref. 7, and in Tables I and II of Ref. 8 for air species. As commented by Hassan and Hash,[9] "For attractive–repulsive potentials, $\sigma_\mu$ and $\sigma_D$ do not have analytical expressions. As a result, the implementation of such a method without introducing simplifying assumptions is not very practical." For instance, for the Lennard-Jones potential, the relations of $\sigma_T$ and $\alpha$ to the relative energy derived from the numerical solutions of $\sigma_\mu$ and $\sigma_D$ were plotted in Fig. 3 of Ref. 7. Indeed, it is not very practical to utilize these profiles in DSMC calculations.

## III. GSS MODEL

In the GSS model, the total cross section and the deflection angle are given by Eqs. (7) and (8), respectively. Therefore, the GSS model may be regarded as an extension of the GHS model for attractive–repulsive potentials, like the VSS model based on the IPL potential is an extension of VHS model. However, the introduction of the soft-sphere scattering law results in a difficulty to determine explicitly the parameters involved in GSS. This issue, essentially important for practical convenience, will be addressed in the following.

It is known that the coefficients of viscosity and self-diffusion of a simple gas, to the first approximation, may be written as[2,3]

$$\mu = \frac{5}{16} \left( \frac{\sqrt{\pi m k T}}{\pi \sigma^2 \Omega^{(2,2)*}} \right), \tag{11}$$

TABLE I. Force constants for the Lennard-Jones (6-12) potential (Ref. 3, Tables 8.4-1 and I-A).

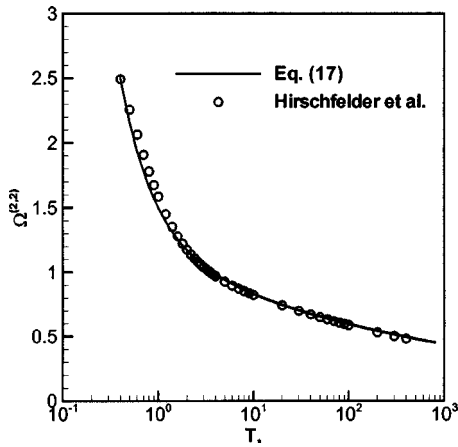| Gas | $\varepsilon/k$ (°K) | $\sigma \times 10^{10}$ m |
|---|---|---|
| He | 10.22 | 2.576 |
| Ne | 35.7 | 2.789 |
| Ar | 124 | 3.418 |
| Kr | 190 | 3.61 |
| Xe | 229 | 4.055 |
| Hg | 851 | 2.898 |
| $H_2$ | 33.3 | 2.968 |
| $D_2$ | 39.3 | 2.948 |
| Air | 97.0 | 3.617 |
| $N_2$ | 91.5 | 3.681 |
| $O_2$ | 113 | 3.433 |
| $F_2$ | 112 | 3.653 |
| $Cl_2$ | 357 | 4.115 |
| $Br_2$ | 520 | 4.268 |
| $I_2$ | 550 | 4.982 |
| CO | 110 | 3.59 |
| $CO_2$ | 190 | 3.996 |
| NO | 119 | 3.47 |
| $N_2O$ | 220 | 3.879 |
| $CH_4$ | 137 | 3.882 |
| $CCl_4$ | 327 | 5.881 |
| $SO_2$ | 252 | 4.290 |

FIG. 1. Comparison of $\Omega^{(2,2)*}$ versus $T_*$. The solid line is given by the fitting formulas (17); the circles are the accurate data for the Lennard-Jones potential (6-12) given in Table I-M, Ref. 3.



FIG. 2. Comparison of $\Omega^{(2,2)*}$ versus $T_*$. The lines (dashed, dotted, and solid) are given by the fitting formulas (17) at $\delta$ of 0.25, 1.00, and 1.75, respectively; the symbols (triangle, square, and circle) are the accurate data for the Stockmayer potential.

$$D = \frac{3kT}{16p}\left(\frac{\sqrt{2\pi kT/m_r}}{\pi\sigma^2\Omega^{(1,1)*}}\right), \qquad (12)$$

with

$$\Omega^{(1,1)*} = \frac{1}{\pi\sigma^2}\int_0^\infty \exp(-\zeta^2)\zeta^5\sigma_D d\zeta, \qquad (13)$$

$$\Omega^{(2,2)*} = \frac{1}{2\pi\sigma^2}\int_0^\infty \exp(-\zeta^2)\zeta^7\sigma_\mu d\zeta, \qquad (14)$$

where $\zeta^2 = \frac{1}{2}m_r c_r^2/kT$, $\sigma_\mu$ and $\sigma_D$ are the viscosity and momentum cross sections, respectively, $p$ and $T$ are the gas pressure and temperature, $m$ is the molecular mass, and $k$ is the Boltzmann constant.

Substituting of Eq. (9) into (13) and (14) yields the self-diffusion and viscosity integrals for the GSS model

$$\Omega^{(1,1)*}_{GSS} = \frac{1}{\pi(\alpha^*+1)}\sum \beta_j^* \Gamma(3-\ell_j^*)T_*^{-\ell_j^*} \qquad (15)$$

and

$$\Omega^{(2,2)*}_{GSS} = \frac{\alpha^*}{\pi(\alpha^*+1)(\alpha^*+2)}\sum \beta_j^* \Gamma(4-\ell_j^*)T_*^{-\ell_j^*}, \qquad (16)$$

where $T_* = kT/\varepsilon$, and $\Gamma(...)$ denotes the gamma function.

## IV. DETERMINATION OF THE PARAMETERS IN GSS

### A. $\alpha^*$, $\beta_1$, $\beta_2$, $\ell_1$, and $\ell_2$

A simple means to determine the parameters of the GSS model is to compare the right-hand sides of Eqs. (15) and (16) against those of (13) and (14), if the latter may be solved analytically. Such analytical solutions are available, however, only at special conditions such as IPL or the hard-sphere scattering law. For the Lennard-Jones (6-12) potential, $\Omega^{(2,2)*}$ was numerically solved by Hirschfelder, Curtiss, and Bird and tabulated as functions of $T_* = kT/\varepsilon$ from 0.3 to 400 in Table I-M, Ref. 3. This paper employs a two-term fitting formula
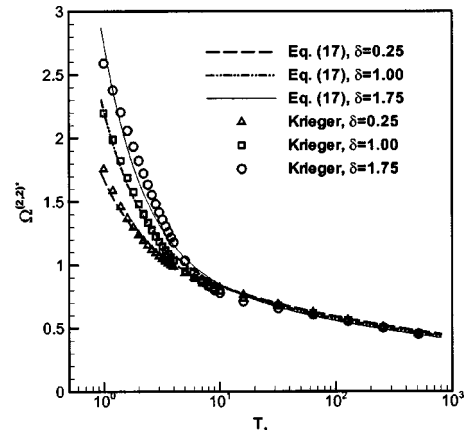
$$\Omega^{(2,2)*}_{fit} = a_1 T_*^{-c_1} + a_2 T_*^{-c_2}, \qquad (17)$$

with $a_1 = 1.1$, $a_2 = 0.4$, $c_1 = 0.133$, and $c_2 = 1.25$. Comparison between the formula (17) and the accurate solution of Hirschfelder et al.[3] shows remarkable agreement (Fig. 1).

The fitting formula (17) is also suitable to the Stockmayer potential. $c_1$ and $c_2$ remain unchanged, whereas $a_1$ and $a_2$ need an additional term to include the polarization effect

$$a_1 = 1.1 - 0.044\delta, \qquad (18)$$

$$a_2 = 0.4 + 0.76\delta. \qquad (19)$$

As shown in Fig. 2, Eq. (17), with $a_1$ and $a_2$ calculated by (18) and (19), compares well with the accurate solution of $\Omega^{(2,2)*}$ for the potential (2) that was obtained by Krieger[10] and included in Table IX, Ref. 3.

Equating the right-hand sides of Eqs. (16) and (17) yields

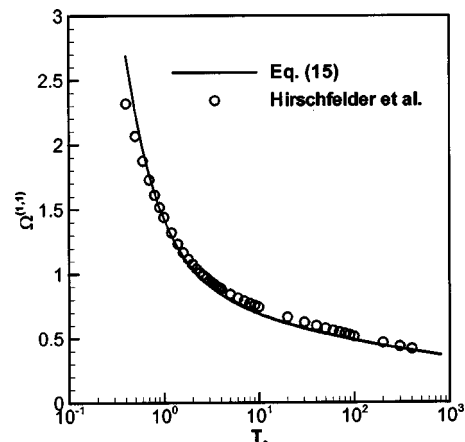$$\ell_1^* \equiv c_1 = 0.133, \qquad (20)$$



FIG. 3. Comparison of $\Omega^{(1,1)}$ versus $T_*$. The solid line is given by the GSS model, i.e., Eq. (15) with the parameters determined by Eqs. (20), (21), and (24)–(26); the circles are the accurate data for the Lennard-Jones (6-12) potential given in Table I-M (Ref. 3).

TABLE II. Parameter for the Stockmayer potential (Ref. 3, Table 8.6-1).

| Gas | $\varepsilon/k$ (°K) | $\sigma \times 10^{10}$ m | $\delta$ |
|---|---|---|---|
| NO | 112.4 | 3.508 | 0.003 371 |
| CO | 109.9 | 3.585 | 0.009 830 |
| $CHCl_3$ | 415.2 | 5.117 | 0.071 77 |
| $H_2S$ | 221.1 | 3.733 | 0.2739 |
| HCl | 218.0 | 3.506 | 0.4123 |
| $SO_2$ | 191.4 | 4.341 | 0.5995 |
| NOCl | 205.2 | 4.332 | 0.7272 |
| $CH_3Cl$ | 243.6 | 4.076 | 0.7606 |
| $CH_3OH$ | 194.9 | 4.082 | 0.7715 |
| $CH_3COCH_3$ | 158.4 | 5.485 | 1.1253 |
| $NH_3$ | 146.8 | 3.441 | 1.2499 |
| $H_2O$ | 230.9 | 2.824 | 2.333 |

$$\ell_2^* \equiv c_2 = 1.25, \tag{21}$$

$$\frac{\alpha^*}{\pi(\alpha^*+1)(\alpha^*+2)} \times \beta_1^* \Gamma(4-\ell_1^*) \equiv a_1, \tag{22}$$

$$\frac{\alpha^*}{\pi(\alpha^*+1)(\alpha^*+2)} \times \beta_2^* \Gamma(4-\ell_2^*) \equiv a_2, \tag{23}$$

and $\beta_j^* \equiv 0$ for $j>2$. This indicates that the first two terms of the general form (7) is enough for either Lennard-Jones or Stockmayer potential.

Another relation to determine $\alpha^*$, $\beta_1^*$, and $\beta_2^*$ may be provided by matching $\Omega_{GSS}^{(1,1)*}$ to the accurate solution of $\Omega^{(1,1)*}$ for the Lennard-Jones (6-12) potential also given in Table I-M, Ref. 3. They agree with each other when (Fig. 3)

$$\alpha^* = 1.5. \tag{24}$$

This value is reasonable since $\alpha^*$ generally lies between 1 and 2 (cf. Ref. 1, p. 42). From Eqs. (22)–(24), we have

$$\beta_1^* = 3.962 - 0.158\delta \tag{25}$$

and

$$\beta_2^* = 4.558 + 8.660\delta. \tag{26}$$

### B. $\varepsilon$, $\sigma$, and $\delta$

The parameters $\varepsilon$, $\sigma$, and $\delta$ in the potentials (1) and (2) for like molecules may be determined from experimental data of coefficient of viscosity. A procedure was described in detail in Ref. 3 that also provided the values of $\varepsilon$, $\sigma$, and $\delta$ for many gases in Tables 8.4-1, 8.6-1, and I-A. Those for common gases are included here (Tables I and II).

Force constants between unlike molecules, in principle, may be obtained from the binary diffusion coefficient at different temperatures. However, few measurements of this sort have been made practically. It is customary to make use of the combining laws that relate the force constants between unlike molecules to those between like molecules.[3] If both unlike molecules are nonpolar or polar, the combining laws are simply as

$$\sigma_{ij} = \frac{\sigma_i + \sigma_j}{2}, \tag{27}$$

$$\varepsilon_{ij} = \sqrt{\varepsilon_i \varepsilon_j}, \tag{28}$$

$$\delta_{ij} = \sqrt{\delta_i \delta_j}. \tag{29}$$

The interaction between a polar molecule and a nonpolar molecule obeys the potential between two nonpolar molecules, i.e., the Lennard-Jones (6-12) potential, whereas the combining laws to decide the force constants become a little different[3]

$$\sigma_{np} = \tfrac{1}{2}(\sigma_n + \sigma_p)\xi^{-1/6}, \tag{30}$$

$$\varepsilon_{np} = \sqrt{\varepsilon_n \varepsilon_p}\xi^2 \tag{31}$$

and

$$\xi = 1 + 0.5\alpha_n \sigma_n^{-3} \delta \sqrt{\varepsilon_p/\varepsilon_n}, \tag{32}$$

where $\sigma_n$, $\varepsilon_n$ are Lennard-Jones potential parameters for the nonpolar molecule, $\sigma_p$, $\varepsilon_p$ are Stockmayer potential parameters for the polar molecule, and $\alpha_n$ is reduced polarizability of the nonpolar molecule. The values of $\alpha_n$ for many gases were given in Table 13.2-3, Ref. 3, and those for common gases included in Table III.

## V. COMPARISON OF MODELS WITH EXPERIMENT

A number of experiments have been carried out to measure transport coefficients. The measured data obtained by different authors covered a wide temperature range, and were collected in Chapter 8, Ref. 3 and Table 6-177, Ref. 11.

In the GSS model, coefficients of viscosity, self-diffusion and diffusion are given by Eqs. (11), (12), (15), and (16), while the parameters $\alpha^*$, $\beta_1$, $\beta_2$, $\ell_1$, and $\ell_2$ involved are calculated by Eqs. (20), (21), and (24)–(26), and the parameters $\varepsilon$, $\sigma$, and $\delta$ for unlike molecules by the combining laws (27)–(29) or (30)–(32). The same procedure applies to the GHS model, except for the value of $\alpha^*$ that becomes unity rather than 1.5.

Coefficients of viscosity and self-diffusion for the VSS and VHS models based on the IPL potential are related as follows:[7]

$$\mu_{VSS} = \mu_{VSH}/S_\mu, \tag{33}$$

$$D_{VSS} = D_{VSH}/S_D, \tag{34}$$

with

$$\mu_{VHS} = \mu_{ref}(T/T_{ref})^\omega, \tag{35}$$

TABLE III. Polarization of molecules (Ref. 3, Table 13.2-3).

| Gas | $H_2$ | $N_2$ | $O_2$ | $Cl_2$ | $N_2O$ | CO | $CO_2$ | $CH_4$ | $CCl_4$ | $SO_2$ |
|---|---|---|---|---|---|---|---|---|---|---|
| $\alpha_n \times 10^{30}$ $m^3$ | 0.79 | 1.76 | 1.60 | 4.61 | 3.00 | 1.95 | 2.65 | 2.60 | 10.5 | 3.72 |
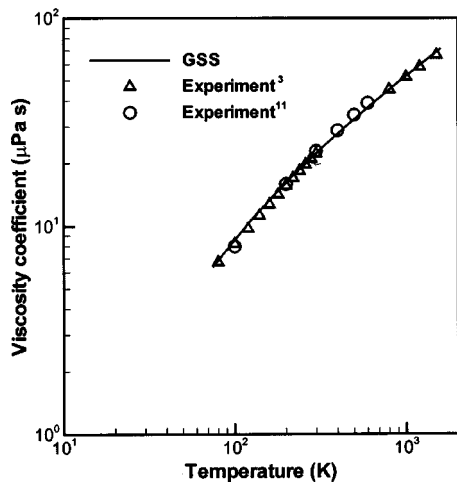
FIG. 4. Comparison of viscosity coefficient of argon given by GSS and experiment.



FIG. 6. Comparison of viscosity coefficient of water vapor (steam) given by GSS model and experiment.

$$D_{VSH} = \frac{2(3.5 - \omega)p}{5kT} \mu_{VSH}, \tag{36}$$

where $\mu_{ref}$ is the reference viscosity at a reference temperature. The values of $\mu_{ref}$, $\omega$ and $\alpha$ depend upon the chemical species, and are given in Tables A1 and A4 of Ref. 1, and Table I of Ref. 7. Although the VSS model is generally applicable to any potential in a mathematical sense, the parameters involved are provided only for the IPL potential.[7,8] Therefore, our discussion on the VSS model limits the IPL situation.

## A. Coefficient of viscosity

The viscosity coefficients of argon and nitrogen given by the GSS model and experiment are compared in Figs. 4 and 5, respectively. The experimental data are available over temperature ranges of 80–1500 K for argon, and 100–1500 K for nitrogen. The GSS and experimental results are in excellent agreement over the entire range of temperature. The coefficients of viscosity between GHS and GSS are only
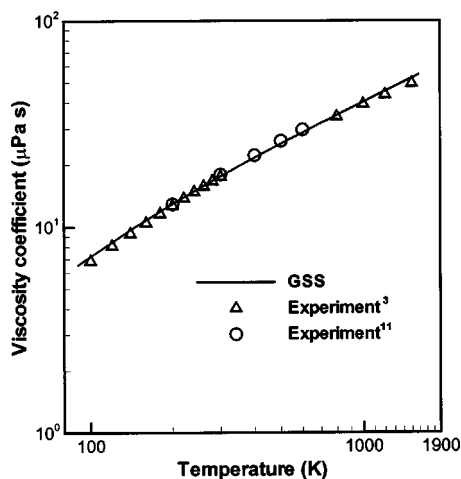


FIG. 5. Comparison of viscosity coefficient of nitrogen given by GSS and experiment.
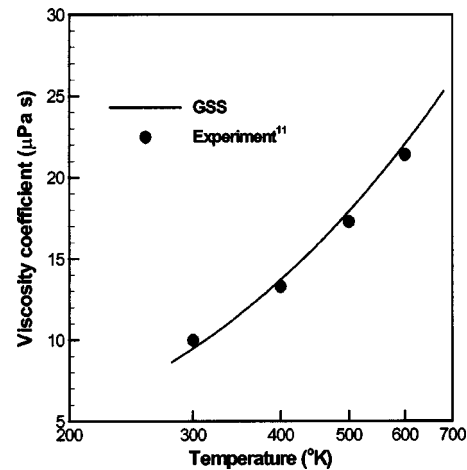
different by a factor of $\alpha^*/[(\alpha^* + 1)(\alpha^* + 2)]$. This factor is equal to 1/6 for GHS ($\alpha^* = 1$), and 6/35 for GSS ($\alpha^* = 1.5$). Therefore, the GHS profiles, not shown in the figures, almost overlay with the GSS profiles. The coefficients of viscosity given by VSS and VHS are close, since the values of $S_\mu$ are equal to 1.023 for argon and 1.029 for nitrogen. The VHS and VSS results agree well with the experimental data at a normal temperature range between 150 and 1000 K, but show an obvious difference at the low and high temperatures. For example, the viscosity coefficients ($\mu$Pa s) for argon given by VHS and VSS are 83.9 and 82.2 at 1500 K, respectively, in comparison with the GSS value of 68.5 and the experimental data[3] of 66.4. The difference up to about 20% may attribute to the attractive portion of molecular interaction neglected in IPL and a constant of $\omega$ employed in VHS and VSS. It is known that the attractive force becomes important at low temperature, and the real value of $\omega$ markedly varies with the range of temperatures (cf. Ref. 2, p. 231). For convenience of engineering simulation, however, the VHS and VSS models employ a constant of $\omega$ that is usually determined at a reference temperature of 273 K. This value is suitable within the neighborhood, i.e., normal temperatures, but it becomes inaccurate at distant temperatures.

Figure 6 compares the coefficients of viscosity of water vapor given by GSS and experiment.[11] As can be seen, there is remarkable agreement. Because of a strong polar property ($\delta = 2.333$), water vapor behaves abnormally from common gases such as argon and nitrogen. Therefore, IPL and Lennard-Jones potentials are not suitable to this kind of molecules,[2,3] so are the VHS, VSS, and GHS models based on them.

## B. Coefficient of self-diffusion

Table IV compares self-diffusion coefficients for four common gases (Ar, $H_2$, $N_2$, and $CO_2$) given by the models and experiment.[3] The GSS results agree quite nicely with the measured data, with a difference generally within 5%, except at an extremely low temperature of 20 K for hydrogen where it is nearly 10%. The difference between the VSS model based on IPL and the experiment is within 10% at the normal

TABLE IV. Comparison of self-diffusion coefficients ($cm^2\ s^{-1}$) at 1 atm given by the GSS, GHS, VSS, VHS models, and experiment.

| Gas | T (°K) | GSS | VSS | GHS | VHS | Experiment (Ref. 3) |
|---|---|---|---|---|---|---|
| Ar | 77.7 | 0.0130 | 0.0178 | 0.0104 | 0.0134 | 0.0134±0.0002 |
|  | 273.2 | 0.161 | 0.173 | 0.129 | 0.131 | 0.156±0.002 |
|  | 353.2 | 0.258 | 0.276 | 0.206 | 0.207 | 0.249±0.003 |
| H₂ | 20.4 | 0.0100 | 0.0165 | 0.008 | 0.0140 | 0.008 16±0.0002 |
|  | 85. | 0.172 | 0.179 | 0.138 | 0.152 | 0.172±0.008 |
|  | 273. | 1.327 | 1.255 | 1.062 | 1.067 | 1.285±0.002 |
| N₂ | 77.7 | 0.0160 | 0.0205 | 0.0128 | 0.0164 | 0.0168±0.0003 |
|  | 273.2 | 0.181 | 0.183 | 0.145 | 0.146 | 0.185±0.006 |
|  | 353.2 | 0.287 | 0.286 | 0.230 | 0.228 | 0.287±0.009 |
| CO₂ | 194.8 | 0.0478 | 0.0557 | 0.0382 | 0.0375 | 0.0516 |
|  | 273.2 | 0.0938 | 0.1069 | 0.0750 | 0.0720 | 0.0970 |
|  | 312.8 | 0.1218 | 0.1389 | 0.0974 | 0.0935 | 0.1248 |
|  | 362.6 | 0.1614 | 0.1847 | 0.129 | 0.1244 | 0.1644 |

temperatures, but it increases significantly at lower temperatures. The hard-sphere scattering law employed in the VHS and GHS models make their results generally more than 20%–30% deviate from the experimental data.

## C. Coefficients of diffusion

Table V compares the coefficients of diffusion of nonpolar molecules given by GSS, VSS, and experiment.[3] In the VSS model, the diffusion coefficients may be written as[1]

$$D_{12} = \frac{3(\alpha_{12}+1)\sqrt{\pi}(2kT/m_r)^{\omega_{12}}}{16\Gamma(3.5-\omega_{12})n(\sigma_{T,\mathrm{ref}})_{12}c_{r,\mathrm{ref}}^{2(\omega_{12}-0.5)}}. \qquad (37)$$

The parameters of $\alpha_{12}$ and $\omega_{12}$ for $N_2$–$H_2$, $N_2$–$CO_2$, $H_2$–$CO_2$ are given in Table I of Ref. 7, and the reference diameter $(d_{\mathrm{ref}})_{12}$ is assumed to be the mean value of those for the pure substances 1 and 2 given in Table A3, Ref. 1. Generally, the three results agree with each other; in details, the GSS results agree better with the measured data.

Table VI includes the coefficients of diffusion for polar molecule of water vapor and nonpolar molecules given by the GSS model and experiment.[3] Again, comparison shows satisfactory agreement.

TABLE V. Comparison of diffusion coefficients ($cm^2\ s^{-1}$) at 1 atm given by GSS, VSS, and experiment.

| Gas | T (°K) | GSS | VSS | Experiment (Ref. 3) |
|---|---|---|---|---|
| N₂–H₂ | 273.2 | 0.696 | 0.712 | 0.674 |
|  | 288.2 | 0.764 | 0.783 | 0.743 |
|  | 293.2 | 0.787 | 0.808 | 0.76 |
| N₂–CO₂ | 273.2 | 0.134 | 0.120 | 0.144 |
|  | 288.2 | 0.148 | 0.131 | 0.158 |
|  | 293.2 | 0.153 | 0.135 | 0.16 |
|  | 298.2 | 0.157 | 0.139 | 0.165 |
| H₂–CO₂ | 273.2 | 0.571 | 0.526 | 0.550 |
|  | 288.2 | 0.628 | 0.580 | 0.619 |
|  | 293.2 | 0.648 | 0.599 | 0.60 |
|  | 298.2 | 0.667 | 0.618 | 0.646 |

TABLE VI. Coefficient of diffusion ($cm^2\ s^{-1}$) for $H_2O$ and nonpolar gases at 1 atm.

| Gas | T (°K) | GSS | Experiment (Ref. 3) |
|---|---|---|---|
| H₂O–H₂ | 307.4 | 1.00 | 1.02 |
|  | 328.5 | 1.13 | 1.12 |
|  | 352.2 | 1.28 | 1.20 |
| H₂O–CO₂ | 307.4 | 0.198 | 0.202 |
|  | 328.5 | 0.225 | 0.211 |
|  | 352.2 | 0.258 | 0.241 |
| H₂O–He | 307.4 | 1.00 | 0.90 |
|  | 328.5 | 1.12 | 1.01 |
|  | 352.2 | 1.26 | 1.12 |
| H₂O–N₂ | 307.4 | 0.272 | 0.256 |
|  | 328.5 | 0.309 | 0.303 |
|  | 352.2 | 0.352 | 0.359 |

## VI. CONCLUSIONS

The GSS model provided a universal procedure to incorporate the Lennard-Jones (6-12) potential for nonpolar molecules and the Stockmayer potential for polar molecules into the DSMC method. The fitting formula (17) played an important role in determining explicitly the parameters involved in GSS. The parameters of the potentials (1) and (2) for a number of gases achieved by kinetic studies for many years,[2,3] together with the combining laws used in kinetic theory to obtain the potential parameters of unlike molecules from those of like molecules, exactly applied to the GSS model. Therefore, it was convenient to implement this model in an engineering simulation. Coefficients of viscosity, self-diffusion and diffusion given by the GSS model agreed well with experimental data for a number of nonpolar and polar gases over a wide range of temperature. Judged by the accuracy and scope of application, the GSS model may be preferable to the previous models.

## ACKNOWLEDGMENTS

## APPENDIX: IMPLEMENTATION OF THE GSS MODEL IN MONTE CARLO SIMULATION

In the DSMC method the collision probability of a pair of molecules within the same cell or sub-cell is proportional to the product of the total cross section $\sigma_T$ and the relative speed. In the GSS model, $\sigma_T$ is easily calculated using Eq. (7), with $\ell_1^*$, $\ell_2^*$, $\alpha^*$, $\beta_1^*$, and $\beta_2^*$ determined by Eqs. (20), (21), and (24)–(26), and $\varepsilon$, $\sigma$, and $\delta$ given in Tables I–III.

According to collision dynamics, in a Cartesian coordinate system, the components of the post-collision relative speed $c_r^*$ may be written as[1]

$$u_r^* = \cos\chi u_r + \sin\chi \sin\varepsilon \sqrt{v_r^2 + w_r^2}, \qquad (A1)$$

$$v_r^* = \cos\chi v_r + \sin\chi(c_r w_r \cos\varepsilon - u_r v_r \sin\varepsilon)/\sqrt{v_r^2 + w_r^2}, \qquad (A2)$$

$$w_r^* = \cos \chi \, w_r - \sin \chi (c_r v_r \cos \varepsilon + u_r w_r \sin \varepsilon)/\sqrt{v_r^2 + w_r^2}, \tag{A3}$$

with

$$\cos \chi = 2 \cdot R_1^{1/\alpha} - 1, \tag{A4}$$

$$\varepsilon = 2\pi \cdot R_2, \tag{A5}$$

where $R_1$ and $R_2$ are random numbers uniformly distributed between 0 and 1, and $u_r$, $v_r$, and $w_r$ are the components of $c_r$.

[1] G. A. Bird, *Molecular Gas Dynamics and the Direct Simulation of Gas Flows* (Clarendon, Oxford, 1994).

[2] S. Chapman and T. G. Cowling, *The Mathematical Theory of Non-uniform Gases* (Cambridge University Press, Cambridge, 1970).

[3] J. O. Hirschfelder, C. F. Curtiss, and R. B. Bird, *Molecular Theory of Gases and Liquids* (Wiley, New York, 1954).

[4] G. A. Bird, "Monte Carlo simulation in an engineering context," in *Rarefied Gas Dynamics*, edited by S. S. Fisher (AIAA, New York, 1981), Part 1, p. 239.

[5] G. A. Bird, "Definition of mean free path for real gases," Phys. Fluids **26**, 3222 (1983).

[6] K. Koura, H. Matsumoto, and T. Shimada, "A test of equivalence of the variable-hard-sphere and inverse-power-law models in the direct-simulation Monte Carlo method," Phys. Fluids A **3**, 1835 (1991).

[7] K. Koura and H. Matsumoto, "Variable soft sphere molecular model for inverse-power-law or Lennard-Jones potential," Phys. Fluids A **3**, 2459 (1991).

[8] K. Koura and H. Matsumoto, "Variable soft sphere molecular model for air species," Phys. Fluids A **4**, 1083 (1992).

[9] H. A. Hassan and D. Hash, "A generalized hard-sphere model for Monte Carlo simulation," Phys. Fluids A **5**, 738 (1993).

[10] F. J. Krieger, "The viscosity of polar gases," Project Rand Report RM-646 (1951).

[11] D. R. Lide, *CRC Handbook of Chemistry and Physics* (CRC, New York, 1999–2000).